Advanced Mathematical Models & Applications
Vol.6, No.2, 2021, pp.106-112

THE EFFECT OF ELASTIC STRAIN OF A THREE-AXIS GYROSTABILIZED PLATFORM ON THE ORIENTATION ACCURACY OF THE SENSITIVITY AXES OF THE INTEGRATING GYROSCOPES: EXPERIMENTAL EVALUATION

A.N. Belyaev[1,2], **A.A. Golozin**[1], **S.A. Shevchenko**[1*]

[1]JSC Command devices research institute, Saint-Petersburg, Russia
[2]Baltic State Technical University "VOENMEH" named after D.F. Ustinov, Saint-Petersburg, Russia

Abstract. The paper considers the experimental evaluation of the effect caused by the elastic strain of the structural members of a three-axis gyro stabilized platform on the orientation accuracy of the sensitivity axes of integrating gyroscopes installed on the platform. The evaluation was carried out in two stages. First, the estimate was calculated with the use of the finite-element modelling. The experimental studies were conducted at the second stage. The results of the comparison of the obtained values are given.

Keywords: space technology, command complexes, three-axis gyrostabilized platform, accuracy, elastic strain, linear accelerations.
AMS Subject Classification: 74S05.
Corresponding author: Sergei, Shevchenko, JSC Command devices research institute, Saint-Petersburg, Russia, e-mail: *shevchenko.sergei.a@yandex.ru*
Received: 30 April 2021; Revised: 29 May 2021; Accepted: 3 July 2021; Published: 24 August 2021.

1 Introduction

Different types of command complexes (CC) are currently widely used in spacecraft control systems (Ishlinskii, 1976; Raspopov et al., 2018). This paper considers a CC based on three-axis gyrostabilizers (Ishlinskii, 1976; Alexandrov, 2008; Lysov, 2009), the mechanical basis of which is a gyrostabilized platform (GSP) with three integrating gyroscopes (IG) of linear accelerations installed on it and three two-degree-of-freedom gyro units (GU) in a three-axis gimbal. Three command angle sensors and three pairs of stabilization motors are installed along the axes of the GSP gimbal. The main functions of the CC included in the control system are the following:

- measurement of information on the projections of the vehicle apparent velocity on the axes of the reference coordinate system (RCS) OX_0,Y_0,Z_0 (Figure 1) and its output to the control system in order to form the functional of the spacecraft centre-of-mass motion control;
- provision for the RCS orientation, invariable relative to the inertial space;
- output of information about the spacecraft attitude relative to the RCS X_0, Y_0, Z_0 to the control system.

Obviously, in this case, the quality of the spacecraft control will significantly depend on the accuracy of its body-fixed RCS formation. The RCS formation process is directly related to accounting various errors are caused by the distinction between real design of CC and an ideal

model. The special error mathematical models of CC are created for taking these distinctions into account. The structures of such models essentially depend on types of CC and usage environments (Kuleshov et al., 2017; Zhukova et al., 2007; Kozlova et al., 2018). The necessity of taking elastic strains influence on accuracy of forming RCS into account is considered in this article.

2 Accuracy of the RCS formation

For the class of CC developed in the Research Institute of Command De-vices, the RCS OX_0, Y_0, Z_0 is determined by the specified orientation of the IG axes of sensitivity (AS) (Figure 1) as follows:

- OX_0, Z_0 is the plane that forms angles α_2, β_2 with the directions of IG_α AS and IG_β AS, respectively;
- OX_0, Y_0 is the plane normal to the plane OX_0, Z_0 that forms angle α_1 with the projection of IG_α AS;
- Y_0, Z_0 is the plane normal to the planes OX_0, Z_0 and OX_0, Y_0.

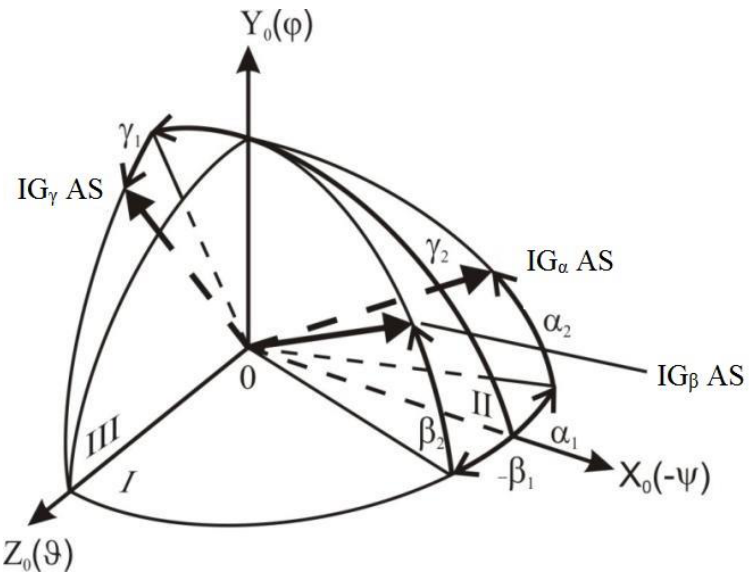

Figure 1: Reference coordinate system

In this case, the accuracy of the RCS formation significantly depends on the errors in the preset values of angles α_i, β_i, γ_i For the CC used in control systems of spacecraft moving with small linear accelerations, the model of IG AS orientation angles in the RCS OX_0, Y_0, Z_0 can be represented as:

$$\alpha_2 = \alpha_2^0; \tag{1}$$

$$\beta_2 = \beta_2^0; \tag{2}$$

$$\alpha_1 = \alpha_1^0; \tag{3}$$

$$\beta_1 = \beta_1^0 + \Delta\beta_1^0; \tag{4}$$

$$\gamma_2 = \gamma_2^0 + \Delta\gamma_2^0; \tag{5}$$

$$\gamma_1 = \gamma_1^0 + \Delta\gamma_1^0; \tag{6}$$

where α_1^0, α_2^0, β_1^0, β_2^0,γ_1^0, γ_2^0 are the calculated values of the IG AS orientation angles in the RCS OX_0, Y_0, Z_0; $\Delta\beta_1^0$, $\Delta\gamma_1^0$, $\Delta\gamma_2^0$ are the IG AS orientation errors in the RCS OX_0, Y_0, Z_0 recorded at the CC manufacturing stage in terrestrial conditions.

However, when CC are used for spacecraft moving with large linear accelerations, this model of the IG AS orientation may be insufficient because in this case we should take into account the effect of elastic strains of the CC structure, in particular, those of the GSP. There will be a change in the design angles of the IG mounting planes that will lead to the AS deflection, which in turn will result in non-orthogonality of the RCS axes. Note that this subject-matter has not been adequately studied in the literature. The publications in this field are usually concerned with strains of gyroscopes due to linear accelerations and additional torques caused by those strains (Matveev, 2012; Wrigley et al., 2012) or errors in the alignment of the gyro AS (Golubek, 2015; Zlatkin et al., 2013).

To take into account the above errors, it is proposed to represent the model of the IG AS orientation angles in the RCS OX_0, Y_0, Z_0 in the following form:

$$\alpha_2 = \alpha_2^0 + \Delta\alpha_{2add}; \tag{7}$$

$$\beta_2 = \beta_2^0 + \Delta\beta_{2add}; \tag{8}$$

$$\alpha_1 = \alpha_1^0 + \Delta\alpha_{1add}; \tag{9}$$

$$\beta_1 = \beta_1^0 + \Delta\beta_1^0 + \Delta\beta_{1add}; \tag{10}$$

$$\gamma_2 = \gamma_2^0 + \Delta\gamma_2^0 + \Delta\gamma_{2add}; \tag{11}$$

$$\gamma_1 = \gamma_1^0 + \Delta\gamma_1^0 + +\Delta\gamma_{1add}; \tag{12}$$

where $\Delta\alpha_{iadd}$, $\Delta\beta_{iadd}$, $\Delta\gamma_{iadd}$, $(i = 1, 2)$ are additional errors in the IG AS orientation in the RCS OX_0, Y_0, Z_0 caused by linear accelerations.

Assuming that linear accelerations lead only to elastic strain of the CC structural members, we can write the errors $\Delta\alpha_{iadd}$, $\Delta\beta_{iadd}$, $\Delta\gamma_{iadd}$ as

$$\Delta\alpha_{iadd} = k_{\alpha i}^{x_0}(n_{x_0} - 1) + k_{\alpha i}^{y_0}(n_{y_0} - 1) + k_{\alpha i}^{z_0}(n_{z_0} - 1); \tag{13}$$

$$\Delta\beta_{iadd} = k_{\beta i}^{x_0}(n_{x_0} - 1) + k_{\beta i}^{y_0}(n_{y_0} - 1) + k_{\beta i}^{z_0}(n_{z_0} - 1); \tag{14}$$

$$\Delta\gamma_{iadd} = k_{\gamma i}^{x_0}(n_{x_0} - 1) + k_{\gamma i}^{y_0}(n_{y_0} - 1) + k_{\gamma i}^{z_0}(n_{z_0} - 1); \tag{15}$$

for n_{x_0}, n_{y_0}, $n_{z_0} > 1$.

Where $k_{\alpha i}^j$, $k_{\beta i}^j$, $k_{\gamma i}^j$ are the gradients of angles per unit of over-load $i = 1, 2, j = x_0, y_0, z_0$. It is the easiest way to represent additional errors $\Delta\alpha_{iadd}$, $\Delta\beta_{iadd}$, $\Delta\gamma_{iadd}$ so that they could be taken into account in the spacecraft control system.

Note that the "physically", the RCS is implemented by the IG and GSP de-signs. Because of this, the effect of the strain of the gimbal structural members on the RCS formation is not considered.

3 Calculating the effect of GSP elastic strains on the RCS formation

To confirm the above assumption as to the possible significance of the effect produced by the GSP elastic strains on the RCS formation, the Research Institute of Command Devices carried out the experimental evaluation to determine the AS deviations of the IG installed on the GSP of one of the previously developed CC.

First, the finite-element modeling in ANSYS was used to compute the values of angle variation gradients under an overload along each of the axes X_0, Y_0, Z_0.

The calculations were performed in a linear elastic formulation for the linear acceleration range from 0 to 40–45g. The finite-element model simulates a GSP with a simulated integrating gyro and gyro unit installed on the GSP trunnions. The model was fixed on spherical surfaces on trunnions with a hinged joint and fixed spherical hinge.

The linear overload was set alternately for each direction of the axes X_0, Y_0, Z_0.

According to the calculation results, it was determined that under the action of large linear accelerations, the error values of the angles α_i, β_i, γ_i may exceed the permissible requirements for the specified parameters by more than 3 times. The obtained high levels of errors required experimental verification.

4 Experimental evaluation of GSP elastic strains. Analysis of the results

Since it is almost impossible to directly measure the changes in the IG AS angles under the action of an overload, we developed a method of indirect verification of the results. The idea is to compare strains of the GPS structure rather than the values of angle variations. In this case, the coincidence of experimental GSP strains with the calculated ones would confirm the correctness of the developed finite-element model, which makes it possible to obtain the variations of the AS orientation angles.

To apply an overload, tests were performed in a centrifuge. The strains at the specified points of the GSP were measured with tensometric equipment.

$BF350\ 3BB\ (11)\ N4-X$ resistance strain gages were installed at the test points in accordance with a half-bridge circuit. The connection corresponds to the option for measuring bending strains. A schematic of the experimental setup is presented in figure 2.

The loading diagram is shown in figure 3. The experimental value of the strains was determined as the difference in the mean-square values of the measurements recorded before the load was applied, and the data obtained under the action of linear accelerations. Each test was repeated 3 times. The frequency of signal registration is 1 Hz.

The tests were carried out on a breadboard that consisted of a GSP on trunnions with mass-and-size evaluation imitators of gyro devices installed on the GSP. In accordance with the computational model, the trunnions had a hinged joint and a fixed hinge. The resulting assembly was mounted on a rigid bracket to be mounted on the centrifuge. The tests were carried out under the action of linear accelerations alternately in the direction of each of the axes X_0, Y_0, Z_0.

As a result of the experiment, we obtained the values of strains at four characteristic points. The term "characteristic point" is used to mean to a point for which the following conditions were fulfilled: the maximum possible distance from stress concentrators and the greatest strains under loading in at least one direction. Thus, four is the maximum number of points on the GPS for which the specified conditions are met. Each measurement was performed in steady state, that is, strain values varied within $\pm$ 1.5 μ/mm over a time interval of 120 s. For this amplitude of strain variation, the minimum possible measured value of the difference between the mean-square values of the data sets was 0.5 $\mu m/m$ State Standard 8.051-81. (2018).

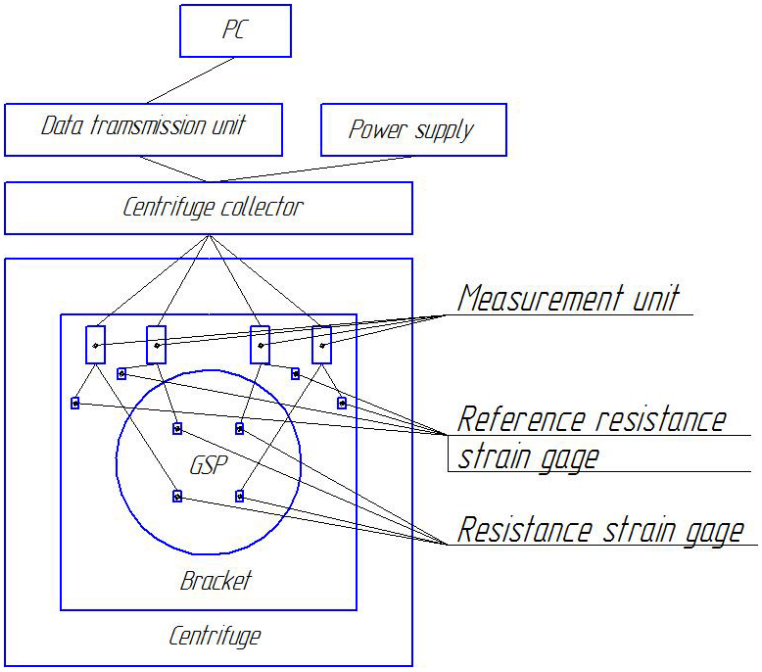

Figure 2: A schematic of the experimental setup

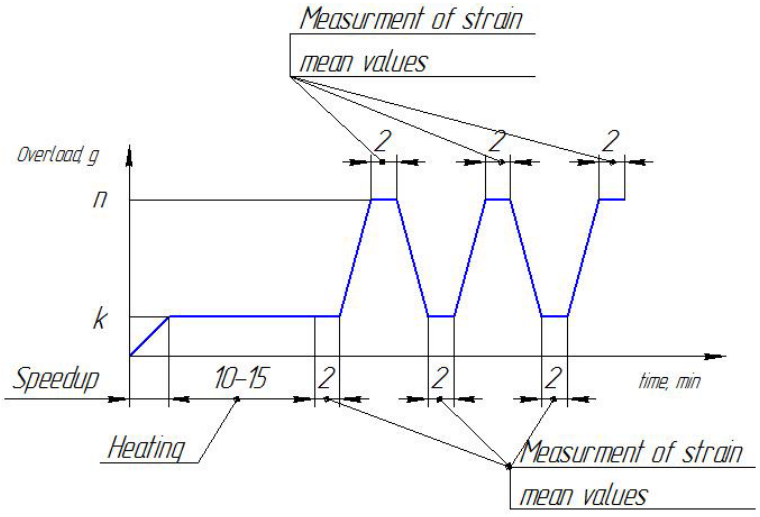

Figure 3: Loading diagram.

The measurement results as well as the calculated values are presented in Tables 1-3.

Table 1: The experimental and calculated values of GSP strains the action of overloading along the X-axis

No.Resistance strain gage	Experimental value of strain, $\mu m/m$	Calculated value of strain, $\mu m/m$
1	43.06	34.57
2	30.32	23.86
3	5.03	8.81
4	55.98	52

Table 2: The experimental and calculated values of GSP strains the action of overloading along the Y-axis.

No.Resistance strain gage	Experimental value of strain, $\mu m/m$	Calculated value of strain, $\mu m/m$
1	43.06	45.38
2	2.03	0.10
3	15.51	9.13
4	0.51	2.81

Table 3: The experimental and calculated values of GSP strains the action of overloading along the Z-axis.

No.Resistance strain gage	Experimental value of strain, $\mu m/m$	Calculated value of strain, $\mu m/m$
1	54.77	50.32
2	7.77	7.86
3	39.90	31.38
4	7.06	2.93

The analysis of the results presented in the tables shows the convergence of the calculated and experimental estimates. Significant difference (more than 25%) between the experimental and the calculated estimates, which are observed in some cases, due to influence of high stress gradient areas on resistance strain gage readings (owing to complex GSP design and different direction of overload action). For instance, there is the resistance strain gage No.4 in high stress gradient area when the overload acts in the direction of Z-axis, but the opposite is true when for the direction of X-axis.

In general, the results of this research confirm the assumption about the significance of the magnitude of IG AS angle variations caused by the elastic strains of the GSP operating under overload conditions and the need to take these errors into account in the mathematical model of the CC errors.

According to the results of the additional measurements, the linear dependence of strains on the overload in the considered range of linear accelerations (0 to 40–45g) was also confirmed. As an example, the graph in figure 4 shows the dependence obtained for one of the strain gages.

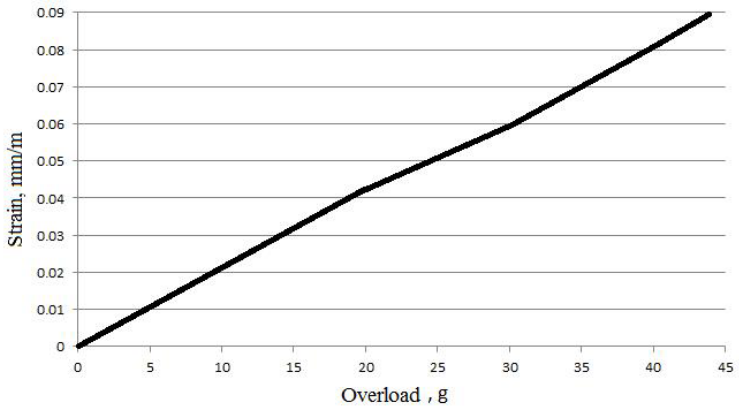

Figure 4: A strain-overload diagram

5 Conclusion

The experimental evaluation was performed to determine additional errors $\Delta\alpha_{iadd}$, $\Delta\beta_{iadd}$, $\Delta\gamma_{iadd}$ caused by elastic strains of the GSP. Analysis of the results has shown that it is necessary to take them into account in the CC error model for certain values of overload. An example is provided to show how to obtain, verify and enter these values into the model.

References

Alexandrov, Yu.S. (2008). Navigation Systems. Part 1. Gyroscopic Sensors and Devices of Navigation Systems. St. Peterburg: BGTU Voenmekh im. D.F. Ustinova (in Russian).

Golubek, V. (2015). Comparison of methods for estimating the effect of errors in a complex of command instruments on the accuracy of launch vehicles with terminal guidance. *Aviation-Space Technics and Technology*, 2, 45-51.

Ishlinskii, A.Y. (1976). *Orientation, Gyroscope and Inertial Navigation.* Moscow. Nauka.

Kozlova, E.S., Rogov, S.V. (2018). The general model of two-axis power gyrostabilizer. International conference *Control Systems for the Electro-Technic Objects* (SYETO-8), Tyla, December, 11-12.

Kuleshov, A.V., Fateev, V.V. (2017). The errors of the biaxial indicator gyrostabilizer of the optical device under the carrier rolling. *Devices and Systems. Control and Diagnostics*, 12, 7-13.

Lysov, A.N. (2009). *Three-axis Powered Gyrostabilizer.* Chelyabinsk, YuUrGU.

Matveev, V.A. (2012). *Gyroscope: It is Simple.* Moscow State Technical University named after N.E. Bauman.

Raspopov, V.Y., Malyutin, D.M. (2018). Measuring instruments and systems for orientation, stabilization and control. *Transactions of the Tulsk State University: Technical Sciences*, 4, 372-386.

Wrigley, W., Hollister, W.M., and Denhard, W.G. (1972). *Gyroscopic Theory, Design, and Instrumentation, Translated into Russian. Kharlamov, S.A.*. Moscow: Mir.

Zhukova, T.A., Mezhiritskiy, E.L., et al. (2017). The influence of the temperate variation of the amplifying and correcting block parameters to the output characteristics and supplies of hardiness of one-axle gyrostabilizer. *Systems and Control Devices, Transactions of NPCAP*, 3, 7-13.

Zlatkin, Yu.M. et al. (2013). Laser strapdown INS for the launch vehicle Tsiklon-4B, *Gyroscope and Navigation, 2*(81), 61-74.

GOST 8.051-81. State system for ensuring uniformity of measurements. Permissible errors in measuring linear dimensions up to 500 mm. (State Standard 8.051-81).